IEEE Photonics Journal
An IEEE Photonics Society Publication

Open Access

Vibration Fiber Sensors Based on SM-NC-SM Fiber Structure

Volume 7, Number 2, April 2015

Yanli Ran
Li Xia
Ya Han
Wei Li
Jalal Rohollahnejad
Yongqiang Wen
Deming Liu

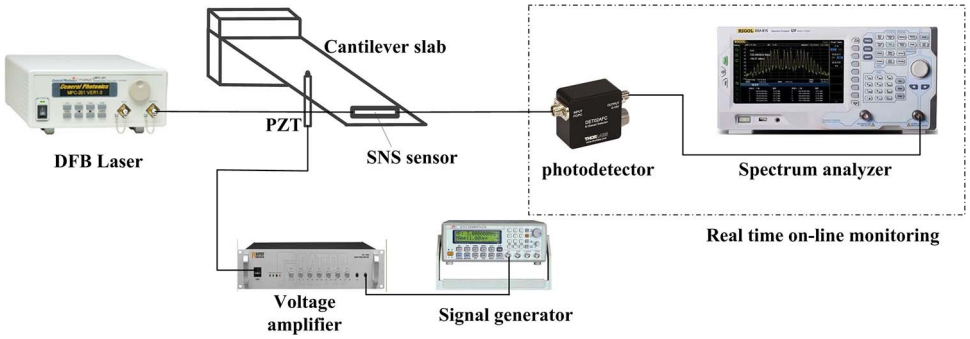

DOI: 10.1109/JPHOT.2015.2408436
1943-0655

IEEE photonics SOCIETY

IEEE

Vibration Fiber Sensors Based on SM-NC-SM Fiber Structure

Yanli Ran, Li Xia, Ya Han, Wei Li, Jalal Rohollahnejad, Yongqiang Wen, and Deming Liu

School of Optical and Electronic Information, Huazhong University of Science and Technology, Wuhan 430074, China

DOI: 10.1109/JPHOT.2015.2408436

Manuscript received January 15, 2015; revised February 21, 2015; accepted February 24, 2015. Date of publication March 3, 2015; date of current version March 10, 2015. This work was supported by the major projects of National Natural Science Fund under Grant 61290315. Corresponding author: L. Xia (e-mail: xiali@hust.edu.cn).

Abstract: A novel vibration sensor based on the single mode (SM)-no core (NC)-SM fiber structure is proposed and experimentally sensing results demonstrated. By numerical simulation, we use an NC fiber (NCF) as the multimode waveguide structure for the multimode interference (MMI) sensing. Through intensity demodulation, the vibration sensing structure can detect continuous vibration disturbances with the frequencies of ranging from 100 Hz to 29 kHz and the inherent frequency of cantilever slab of 700 Hz. The frequency sensing resolution is 1 Hz in real-time monitoring. The proposed compact structure is easy to fabricate and has low cost.

Index Terms: No core fiber (NCF), intensity demodulation, vibration sensing.

1. Introduction

Detection of vibration is widely applied to many fields such as civil infrastructures and environmental surveillance in which the piezoelectric accelerometer is the most conventional vibration sensor. However, it is unsuitable to be applied to the electromagnetic sensitive environment due to the lack of an effective electrical isolation function. Compared with traditional vibration sensors such as piezoelectric accelerometer, fiber optic sensor has many unique advantages, such as immunity to electromagnetic interference, light weight, compact size, multi-functionality, and ability to multiplex [1], [2].

Various fiber optic vibration sensing techniques have been extensively studied, such as hetero-core fiber optics vibration sensors [3], the fiber Bragg grating vibration sensor [4]–[6], and in-fiber Mach–Zehnder interferometers [7]. Nishiyama presented a novel approach to the tunable mechanical vibration measurement using the hetero-core optical fiber optics sensor based on rigid supported beam property. The hetero-core fiber optic vibration sensors could pick up the free vibration from an impact force. In order to obtain a higher detectable frequencies range, the authors designed two configurations and found that the vibration sensor with tension to the fiber enabled its detectable frequencies to be higher than without tension [3]. This kind of low-cost vibration sensor provides a good choice of vibration monitoring in fault diagnosis of the industrial equipment. In [4], Tsuda proposed a fiber Bragg grating vibration-sensing system employing a fiber laser utilizing an FBG sensor as the ring cavity mirror. The sensor could detect vibration over a broad band ranging from a few hertz up to ultrasound, regardless of both the strain and temperature applied to the FBG

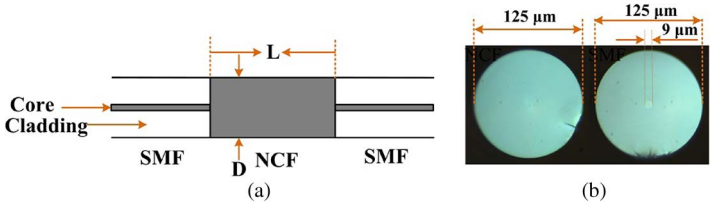

Fig. 1. (a) Schematic of SNS fiber sensor. (b) Metallographic microscope image of cross sections of NCF and SMF structure.

sensor. According to [7], Xu proposed a vibration sensing Mach–Zehnder interferometer using a tapered bend–insensitive fiber, which was presented to realize damped and continuous vibration disturbances ranging from 1 Hz up to 500 kHz. The sensor could detect a large frequency range. However, the fiber optic vibration sensors mentioned above have more complicated structure, high production cost, low sensitivity, and difficult fabrication.

Recently, the fiber optic sensor based on the single mode-multimode-single mode structure which utilizes the multimode interference (MMI) theory has been intensively investigated [8]–[10]. The multimode interference theory has been utilized in the design and fabrication of novel optical devices such as displacement sensors [11], refractometer sensors [12], temperature sensors [13], strain sensors [14], and bandpass filters [15]. In order to improve the detection sensitivity of normal SMS structure, it needs to corrode the multimode fiber (MMF) cladding even the core by various chemical compounds [12]. However, chemical corrosion is not only dangerous but difficult to precisely control, and the corrosive method will lead to the decrease of the fiber mechanical strength and increase of the cutting and welding difficulty. It is difficult to accurately design and fabricate. Li had proposed a simple and compact NCF-FBG interferometer based on MMI theory, for simultaneous measurement of refractive index and temperature, which experimentally demonstrated high surrounding refractive index sensitivity [16]. Li also stated that the multi modes of the no core fiber (NCF) would be excited when the light is launched from single mode fiber (SMF) to the NCF.

In this paper, we propose a novel fiber sensor for vibration sensing based on the SM-NC-SM (SNS) simple structure. By numerical simulation a novel SNS structure is designed and used as vibration sensor based on MMI. The NCF is employed as multimode waveguide with a first and second re-imaging length of circa 14.6 mm and 29.2 mm at 125 μm diameter respectively. In our design we used the second re-imaging length. Section 2 of this paper provides a description about the principle of MMI in the NCF and intensity modulation of this vibration sensing. After that, we demonstrated the experiment and monitored the vibration frequencies in Section 3. The inherent frequency of the setup also could be obtained. The fabrication of such sensors is low cost and straightforward, which provides a promising choice for many applications.

2. Schematic Diagram and Numerical Simulations of the Sensor

The schematic of the sensor is shown in Fig. 1(a). The key component is a section of NCF which is spliced to the lead-in single mode fiber (SMF) and lead-out SMF. NCF is a new kind of optical fiber which only contains solid cladding and coating made of pure fused silica materials and polymer materials, respectively. Fig. 1(b) shows the cross sections of NCF and SMF observed through the metallographic microscope. It can be seen the structure difference between NCF and SMF. The fiber core and cladding of SMF are clearly visible while the NCF showing a solid cladding.

Assuming that the SMFs and NCF are ideally aligned with the circular symmetry of the input field, when the light launched into the lead-in SMF acts as LP_{01} mode, there will be only LP_{01} mode and higher order LP_{0m} modes excited [17] as light injects from SMF to NCF. We will use the amplified spontaneous emission (ASE) source and optical spectrum analyzer to observe the interference spectrum.

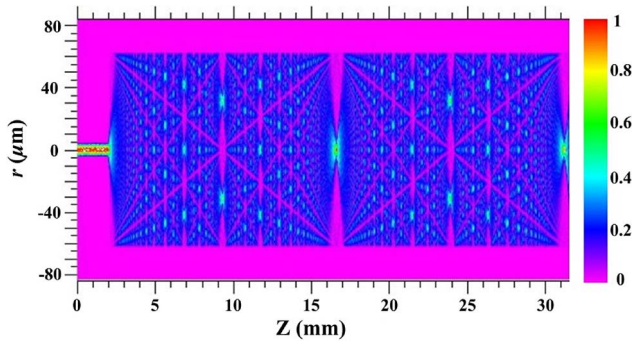

Fig. 2. Light propagation along the NCF at the 1550 nm wavelength.

Defining the field profile of the LP_{0m} as $\psi_m(r)$, where r is the radial coordinate in the cross section of the fiber, the NCF input field can be written as

$$E(r,0) = \sum_{m=1}^{M} b_m \psi_m(r) \tag{1}$$

where b_m is the excitation coefficient of LP_{0m} mode, which can be expressed as

$$b_m = \frac{\int_0^\infty E(r,0)\psi_m(r)rdr}{\int_0^\infty \psi_m(r)\psi_m(r)rdr} \tag{2}$$

Then, the field NCF section at the propagation distance z can be calculated by

$$E(r,z) = \sum_{m=1}^{M} b_m \psi_m(r)\exp(j\beta_m z) \tag{3}$$

where β_m is the propagation constant of the LP_{0m} mode in the NCF.

It can be seen that the NCF section field is determined by r and z. For easy fabrication, the diameter r is selected equal to the SMF cladding diameter 125 μm. Therefore, we need to calculate the optimal length of the NCF with a selected diameter.

In the simulation (using the Rsoft/ beam propagation method (BPM)), the NCF and the surrounding air (cladding) have refractive indices of 1.4446 and 1.0003 respectively. Due to the large difference between the refractive index of NCF and that of the around air, the NCF is equivalent to MMF. The amplitude distribution of the calculated field along the NCF at the 1550 nm wavelength is shown in Fig. 2. The simulation results demonstrate that the first and second re-imaging length within the NCF is circa 14.6 mm and 29.2 mm respectively. For easy splicing and fixation, in our experiment, the parameters of NCF in SNS structure are chosen as following: the length L of NCF is 2.92 cm and the solid cladding diameter D is 125 μm which is equal to the cladding diameter of the SMF.

We used a simple setup to experimentally confirm the simulation results and observe the MMI spectrum of SNS sensor. An ASE broadband source injects light into the SNS structure, and the transmission spectrum is monitored using an optical spectrum analyzer.

As shown in Fig. 3(a), the spectrum can be calculated by subtracting the ASE spectrum from the SNS spectrum. The wavelength range of interference is from 1540 nm to 1600 nm. It can be seen that the interference fringe of the SNS sensor is not uniform and there are multiple peaks and dips on the measured transmission spectra. In Fig. 3(b), the FFT of the transmission power spectrum is shown, that demonstrate the number and power distribution of the LP_{0m} modes in frequency domain. From spatial frequency transmission spectrum, we can find that three main

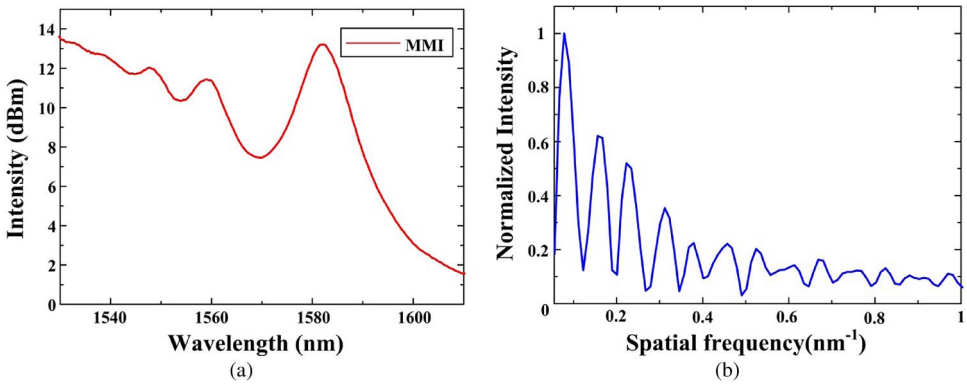

Fig. 3. (a) Measured transmission spectrum and (b) corresponding spatial frequency spectrum of SNS structure.

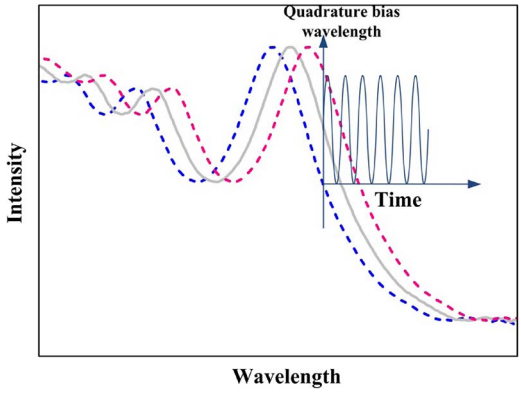

Fig. 4. Schematic illustration of SNS fiber vibration sensing based on the intensity modulation.

frequencies could be extracted. The peaks located at different frequencies exhibits two dominant intensity peaks corresponding to two cladding modes.

The SNS sensor is mounted on a cantilever. When the cantilever vibrates, it will cause a dynamic strain variation on the NCF, and the fiber length will vary with the mechanical strain. Thus it will cause a fluctuation in power spectrum of the SNS structure. If a piezoelectric transducer (PZT) is used to provide a continuous dynamic strain on the NCF by straightly fixing the fiber on it, the transmission spectrum of the SNS sensor will periodically blue shift or red shift when the fiber sensor interference length is compressed or elongated. Thus, the intensity at an interference wavelength will periodically decrease and increase at a vibration frequency. Fig. 4 shows a schematic illustration of SNS fiber vibration sensing based on the intensity modulation. Accordingly, a linear intensity response can be acquired by observing the quadrature bias wavelength when the sensor is vibrated at low amplitude.

3. Experimental Results and Discussions

The experimental setup to utilize an SNS based vibration sensor is shown in Fig. 5. The sensor is fixed straightly to a cantilever slab which is vibrated by standard piezoelectric transducer (PZT) shown in Fig. 6(a). Driven by the periodic sinusoidal signal with a peak to peak voltage of 500 mV shown in Fig. 6(b), the PZT continuously vibrates, sequentially applies the vibration force to the cantilever slab.

As the analysis in part 2, when a vibration applied to the SNS fiber structure, it will cause periodic output intensity variation at an interference wavelength ranging from 1540 nm to 1600 nm. In this experiment, a 1550 nm distributed feed-back laser is employed to emit light into the SNS

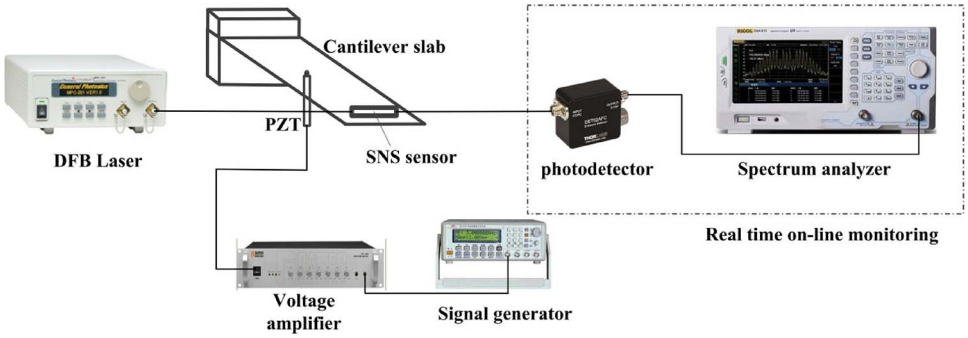

Fig. 5. Schematic setup for SNS vibration sensing.

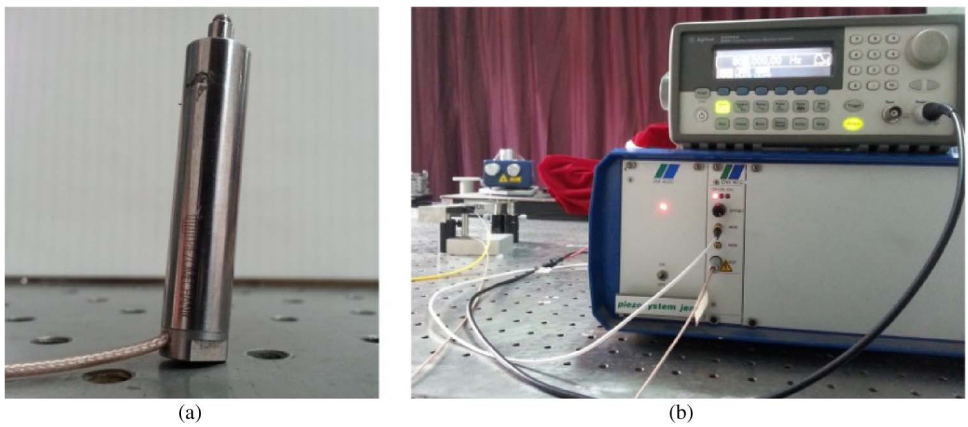

(a) (b)

Fig. 6. (a) Piezoelectric transducer and (b) signal generator and voltage amplifier.

fiber sensor. The high-speed photo detector adopted in the experiment has a spectral range of 830 nm∼2100 nm and a maximum 250 ps rise and fall time. Since the transmitted optical power in the SNS fiber structure is sensitive to the MMI, the photo detector output will reflect the vibration induced power variations, which can be real time monitored by a frequency spectrum analyzer to record the vibration frequencies.

In the frequencies range from 100 Hz to 29 kHz, the vibration frequencies are clearly detectable. A fast Fourier transformation analysis has been carried out on the measured time domain response data by the spectrum analyzer. In the real-time vibration monitoring experiments, the frequency spectra of 100 Hz, 700 Hz, 2 kHz, 10 kHz, 20 kHz, and 29 kHz corresponding to the time domain responses are shown in Fig. 7. As the harmonic energy is loaded on fundamental frequency, the power of higher harmonics with smaller amplitude is less than that of fundamental frequencies with stable peaks. In the experiment, we take the fundamental frequency as the detected frequency. From the frequency spectra in Fig. 7, it can be seen that the fundamental frequencies measured by the SNS vibration sensor are well matched with the applied frequencies. Furthermore the low levels of higher harmonics prove that the sensor does not excessively distort the measured vibration signal. The maximum side-mode suppression ratio (SMSR) of fundamental frequency is ∼50 dB at 700 Hz and the minimum SMSR is ∼15 dB at 29 kHz.

Fig. 8(a) shows the power variations along with the applied frequencies. If the vibration frequencies are less than the inherent frequency of cantilever slab, the amplitude increases with the increasing of applied frequencies. It will induce the rise of output power. Resonance occurs when the vibration frequency is close to the inherent frequency. The amplitude has the maximum peak, and the output power is higher than that of other frequencies. Furthermore the power will decrease when the vibration frequencies are higher than the inherent frequencies.

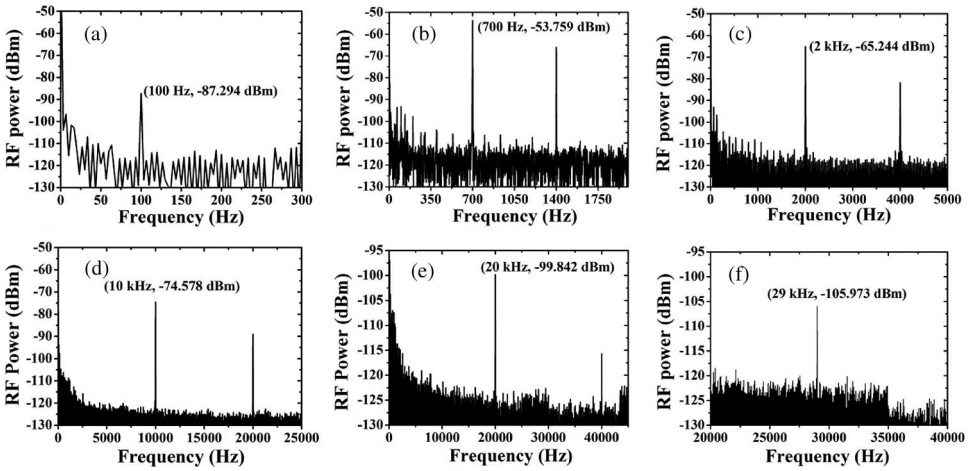

Fig. 7. Measured frequency spectra of the SNS vibration sensor at different frequencies: (a) 100 Hz; (b) 700 Hz; (c) 2 kHz; (d) 10 kHz; (e) 20 kHz; (f) 29 kHz.

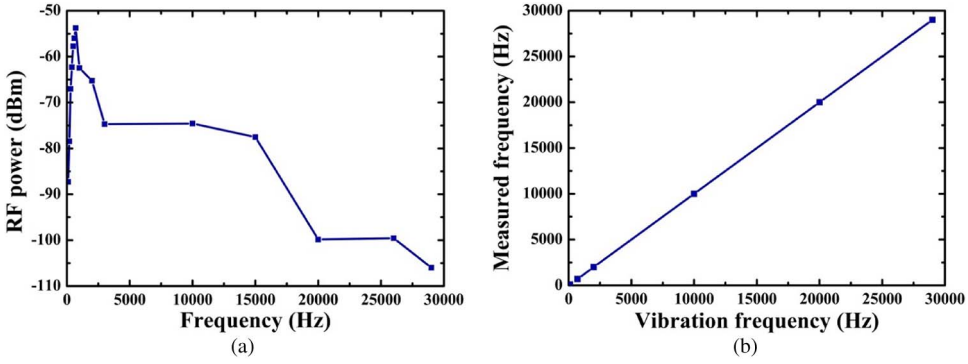

Fig. 8. Curves of (a) the power variations along with frequencies and (b) the measured frequencies vs the vibration frequencies at 100 Hz, 700 Hz, 2 kHz, 10 kHz, 20 kHz, and 29 kHz.

As shown in Fig. 8(a), it can be seen that the inherent frequency of this experimental setup is ~700 Hz.

The resolution of the real time online monitoring can reach 1 Hz. We can see the sensing responses from six randomly chosen frequencies lead to a linear curve in Fig. 8(b). Limited by the PZT modulated speed used in the experiment, this kind of new optical fiber sensor can monitor the highest frequency up to 29 kHz. Compare to [3], both of the vibration fiber sensors have a lower cost and simpler configuration than the FBG vibration–sensing system [4] and vibration sensing Mach–Zehnder interferometer [7]. The hetero–core fiber optics sensor realizes a tunable mechanical vibration measurement with a detectable frequency range of 135–4680 Hz while the SNS sensor detects a large frequency range of 100 Hz–29 kHz in real time monitoring.

4. Conclusion

In summary, a novel fiber vibration sensor based on the SNS structure has been proposed and experimentally demonstrated. By numerical simulation, a section of NCF with precise length is adopted to compose the sensor. Based on the intensity demodulation by monitoring the power fluctuation at an operation wavelength, a high sensitive and rapid response scheme has been designed to detect the vibration frequency in real time monitoring. The experimental results demonstrate that the fiber vibration sensor can detect a frequency range from 100 Hz to 29 kHz

with 1 Hz resolution. The inherent frequency of cantilever slab can be calculated to be 700 Hz by the curve of power variations along with frequencies. This kind of compact fiber sensor provides a good choice for vibration sensing with high sensitivity, simple configuration, and low cost.

References

[1] B. Lee, "Review of the present status of optical fiber sensors," *Opt. Fiber Technol.*, vol. 9, no. 2, pp. 57–79, Aug. 2002.
[2] A. Othonos, "Fiber Bragg gratings," *Rev. Sci.*, vol. 68, no. 12, pp. 4309–4341, Dec. 1997.
[3] M. Nishiyama and K. Watanable, "Frequency characteristics of hetero-core fiber optics sensor for mechanical vibration," *Sens. Actuators A, Phys.*, vol. 209, pp. 154–160, Mar. 2014.
[4] H. Tsuda, "Fiber Bragg grating vibration-sensing system, insensitive to Bragg wavelength and employing fiber ring laser," *Opt. Lett.*, vol. 35, no. 14, pp. 2349–2351, Jul. 2010.
[5] S. Tanaka, H. Somatomo, A. Wada, and N. Takahashi. "Fiber-optic mechanical vibration sensor using long-period fiber grating," *Jpn. J. Appl. Phys.*, vol. 48, no. 7S, Jul. 2009, Art. ID. 07GE05.
[6] T. K. Gangopadhyay. "Prospects for fibre Bragg gratings and Fabry–Perot inter–ferometers in fibre–optic vibration sensing," *Sens. Actuators A.*, vol. 113, no. 1, pp. 20–38, Jun. 2004.
[7] Y. Xu *et al.*, "Vibration sensing using a tapered bend–insensitive fiber based Mach–Zehnder interferometer," *Opt. Exp.*, vol. 21, no. 3, pp. 3031–3042, Feb. 2013.
[8] Q. Wang, G. Farrell, and W. Yan, "Investigation on single mode multimode single mode fiber structure," *J. Lightw. Technol.*, vol. 26, no. 5, pp. 512–519, Mar. 2008.
[9] H. Li *et al.*, "Multimode interference in circular step index fibers studied with the mode expansion approach," *J. Opt. Soc. Amer. B.*, vol. 24, no. 10, pp. 2707–2720, Oct. 2007.
[10] L. B. Soldano and E. C. M. Pennings, "Optical multimode interference devices based on self- imaging: Principles and applications," *J. Lightw. Technol.*, vol. 13, no. 4, pp. 615–627, Apr. 1995.
[11] A. Mehta, W. Mohammed, and E. G. Johnson, "Multimode interference based fiber optic displacement sensor," *IEEE Photon. Technol. Lett.*, vol. 15, no. 8, pp. 1129–1131, Aug. 2003.
[12] Q. Wu, Y. Semenova, P. Wang, and G. Farrell, "High sensitivity SMS fiber structure based refractometer-analysis and experiment," *Opt. Exp.*, vol. 19, no. 9, pp. 7937–7944, Apr. 2011.
[13] R. X. Gao, Q. Wang, F. Zhao, B. Meng, and S. L. Qu, "Optimal design and fabrication of SMS fiber temperature sensor for liquid," *Opt. Commun.*, vol. 283, no. 16, pp. 3149–3152, Aug. 2010.
[14] E. Li, "Sensitivity-enhanced fiber-optic strain sensor based on interference of higher order modes in circular fibers," *IEEE Photon. Technol. Lett.*, vol. 19, no. 16, pp. 1266–1268, Aug. 2007.
[15] W. S. Mohammed, P. W. E. Smith, and X. Gu, "All-fibre multimode interference bandpass filter," *Opt. Lett.*, vol. 31, no. 17, pp. 2547–2549, Sep. 2006.
[16] L. Li *et al.*, "Novel NCF-FBG interferometer for simultaneous measurement of refractive index and temperature," *IEEE Photon. Technol. Lett.*, vol. 24, no. 24, pp. 2268–2271, Dec. 2012.
[17] Y. Chen, Q. Han, T. Liu, and H. Xiao, "Wavelength dependence of the sensitivity of all-fiber refractometers based on the single mode-multimode-single mode structure," *IEEE Photon. J.*, vol. 6, no. 4, Aug. 2014, Art. ID. 6801807.